Review Article

Real-time magnetic resonance imaging of cardiac function and flow—recent progress

Shuo Zhang[1,2], Arun A. Joseph[1,2], Dirk Voit[1], Sebastian Schaetz[1], Klaus-Dietmar Merboldt[1], Christina Unterberg-Buchwald[2,3,4], Anja Hennemuth[5], Joachim Lotz[2,3], Jens Frahm[1,2]

[1]Biomedizinische NMR Forschungs GmbH am Max-Planck-Institut für biophysikalische Chemie, Göttingen 37070, Germany; [2]DZHK (German Cardiovascular Research Center), partner site Göttingen, Göttingen, Germany; [3]Diagnostische und Interventionelle Radiologie, [4]Kardiologie und Pneumologie, Universitätsmedizin Göttingen, Göttingen 37075, Germany; [5]Fraunhofer MEVIS Institute for Medical Image Computing, Bremen, Germany

Correspondence to: Jens Frahm. Biomedizinische NMR Forschungs GmbH am Max-Planck-Institut für biophysikalische Chemie, Göttingen 37070, Germany. Email: jfrahm@gwdg.de.

Abstract: Cardiac structure, function and flow are most commonly studied by ultrasound, X-ray and magnetic resonance imaging (MRI) techniques. However, cardiovascular MRI is hitherto limited to electrocardiogram (ECG)-synchronized acquisitions and therefore often results in compromised quality for patients with arrhythmias or inabilities to comply with requested protocols—especially with breath-holding. Recent advances in the development of novel real-time MRI techniques now offer dynamic imaging of the heart and major vessels with high spatial and temporal resolution, so that examinations may be performed without the need for ECG synchronization and during free breathing. This article provides an overview of technical achievements, physiological validations, preliminary patient studies and translational aspects for a future clinical scenario of cardiovascular MRI in real time.

Keywords: Real-time magnetic resonance imaging (MRI); cardiovascular imaging; cardiac function; blood flow; arrhythmias

Submitted Mar 09, 2014. Accepted for publication May 30, 2014.
doi: 10.3978/j.issn.2223-4292.2014.06.03
View this article at: http://dx.doi.org/10.3978/j.issn.2223-4292.2014.06.03

Cardiovascular disease is the leading cause of death in developed countries (1). Relevant noninvasive diagnostic imaging techniques, which range from echocardiography to X-ray computed tomography, face a most demanding situation due to the need for both high spatial and high temporal resolution. In the past two decades magnetic resonance imaging (MRI) has been established a valuable new tool for studying cardiovascular disease which provides access to anatomic structure and function, blood flow, tissue perfusion and viability (2,3). Cardiovascular MRI is therefore included in national and international guidelines for the clinical evaluation of congenital heart disease, cardiomyopathies, myocardial viability or myocarditis, e.g., see (4,5).

In a technical sense, state-of-art cardiac MRI approaches are mostly based on fast gradient-echo pulse sequences which achieve synthetic "cine" representations of an average cardiac cycle using retrospective electrocardiogram (ECG) gating concepts. On the other hand, cardiac function and flow represent dynamic processes that are affected by a variety of physiologic influences such as respiration, blood pressure, heart rate, exercise, or medication. The underlying myocardial and valvular movements are characterized by only a limited degree of periodicity which is often further compromised in patients with cardiovascular disease. Moreover, ECG-synchronized MRI recordings yield only mean representations of functional parameters as cine image series represent the average of multiple heartbeats and therefore potentially miss useful diagnostic information about beat-to-beat variations in cardiac performance.

These limitations may now be overcome by recent advances in real-time MRI that allow for a direct monitoring

of cardiovascular functions without ECG synchronization and during free breathing. The method proposed here relies on nonlinear inversion (NLINV) reconstructions of highly undersampled gradient-echo MRI datasets and provides series of high-quality images, i.e., MRI movies, with individual imaging times as short as 20 ms (6,7).

This article provides an overview of the NLINV performance and its first applications in the field of cardiovascular imaging. Examples for real-time cardiac MRI cover field strengths of 1.5 T, 3 T and 7 T as well as applications with T1 and steady-state free precession (SSFP) contrast. Complementary, real-time flow studies, which exploit the principles of phase-contrast MRI, address blood flow in major heart vessels including the aorta, superior vena cava, and pulmonary arteries as well as under different physiologic conditions. Preliminary clinical cases demonstrate the future potential of real-time MRI in the diagnosis and management of patients with cardiovascular disease.

Towards real-time cardiovascular MRI

Past and ongoing developments

Since the earliest medical applications of MRI, attempts to further accelerate the imaging process have been a major driving force for technical improvements. Basic achievements that led to reductions in imaging time comprise echo-planar imaging (EPI) (8), low flip-angle gradient-echo imaging [fast low-angle shot (FLASH)] (9,10) and single-shot fast spin-echo imaging [rapid acquisition with relaxation enhancement (RARE)] (11). With respect to cardiac imaging, the FLASH technique efficiently allowed for ECG-triggered acquisitions of the human heart and the reconstruction of cine MRI movies. Later variants primarily focused on gradient-echo sequences with fully-balanced magnetic field gradients which generate a SSFP signal and maximize the contrast between myocardium and blood pool (12,13).

A further substantial progress in MRI acquisition speed was the development of parallel imaging (14-16), later often in conjunction with non-Cartesian encoding strategies such as spiral (17-19) or radial trajectories (20-25). Parallel MRI utilizes the spatially complementary sensitivity profiles of the individual elements of a large array of receive coils. This extra information then allows for a moderate undersampling of the acquired MRI data which translates into a corresponding acceleration of the imaging process (typically by a factor of about two). Applications of parallel imaging to cardiovascular imaging indeed resulted in significant improvements, e.g., see (26,27).

The adaptation of radial encoding schemes turned out to be particularly attractive for cardiac MRI because it eliminates the motion sensitivity normally introduced by conventional phase-encoding gradients. Apart from cross-sectional imaging (24,25,28,29) such applications were mainly described for efficient 3D coverage of the heart (30-33). More recently, parallel imaging variants such as k-t broad-use linear acquisition speed-up technique (BLAST) and k-t sensitivity encoded (SENSE) (34,35) and through-time radial generalized autocalibrating partially parallel acquisition (GRAPPA) (36) were proposed to record movies with high frame rates. These techniques enhance the degree of undersampling by exploiting temporal information, but have to determine the coil sensitivity maps needed for image reconstruction either by a lengthy calibration scan prior to any real-time acquisition, an approach with very limited practical utility, or by extensive data averaging of differently encoded real-time acquisitions over time, which is prone to motion blurring. In fact, both methods do not determine the actual coil sensitivity profiles that correspond to any individual frame of a dynamic image series, and in a mathematical sense therefore compromise the best possible image quality (see below).

Image reconstruction by NLINV

Data acquisition in all modern MRI system embraces the advantages of multiple receive coils such as improved signal-to-noise ratio (SNR) and the ability to accelerate the process by parallel imaging. As a consequence, parallel MRI no longer reconstructs the images by a direct inverse fast Fourier transformation (FFT), but requires an iterative solution to an inverse problem. The reconstruction task involves the determination of both the complex coil sensitivity profiles and the desired image from a number of undersampled datasets. Because the coil sensitivities are unknown and, in a dynamic setting which monitors a moving object, also change during imaging due to dielectric coupling of the conductive tissue with the receive coil elements, the true reconstruction problem in MRI emerges as a NLINV problem, i.e., a simultaneous determination of all coil sensitivities and the image.

This nonlinear aspect is generally ignored in conventional parallel MRI in order to avoid the high computational demand of respective solutions. Instead, commercially available methods either use an initial calibration scan or fully sample the central MRI data to determine low-

Table 1 Experimental parameters for real-time cardiac MRI

Field strength	1.5 T	3 T		7 T
Contrast	SSFP	SSFP	T1	T1
Field-of-view/mm^2	256.00×256.00	256.00×256.00		256.0×256.0
Image matrix size	144.00×144.00	160.00×160.00		208.0×208.0
Resolution/mm^3	1.80×1.80×8.00	1.60×1.60×6.00		1.2×1.2×6.0
Repetition time/ms	2.72	2.80	2.22	2.56
Echo time/ms	1.36	1.40	1.36	1.59
Spokes per image	15.00	11.00	15.00	13.00
Imaging time/ms	40.80	30.80	33.30	33.30
Frame rate/s^{-1}	25.00	32.00	30.00	30.00
Undersampling factor	15.00	23.00	17.00	25.00
Flip angle/degree	35.00	30.00	10.00	10.00
Bandwidth/Hz Pixel^{-1}	1,929.00	1,736.00	1,736.00	1,335.00

MRI, magnetic resonance imaging; SSFP, steady-state free precession.

resolution coil sensitivity maps by inverse FFT. With known coil sensitivities the subsequent reconstruction reduces to an easy-to-solve linear inverse problem. However, what might be acceptable for parallel MRI applications with only moderate degrees of undersampling becomes a limitation for real-time MRI acquisitions with undersampling factors of 20 to 30. In such circumstances, it seems mandatory to solve the true MRI reconstruction problem and jointly estimate all coil sensitivities and the image from all available datasets: This is the basic concept of regularized NLINV as originally described for Cartesian parallel imaging (37).

For dynamic applications the method was extended to arbitrary spatial encoding schemes including highly undersampled gradient-echo sequences with radial trajectories (38). Subsequent developments achieved true real-time imaging with acquisition times as short as 20 ms (6) by exploiting the temporal continuity of a dynamic movement. Temporal regularization to the preceding frame of an image series adds prior knowledge to the ill-conditioned NLINV reconstruction and effectively constrains the range of possible solutions, i.e., image estimates. In theory, the results not only represent the best possible reconstructions, but also lead to a fully self-consistent technique in the sense that only the actual dataset but no preceding calibration scan or any other supplementary information is required for serial reconstructions of individual images.

Recent developments of the NLINV method validated its spatiotemporal fidelity with the use of a specially designed motion phantom (39) and evaluated the advances of incorporating an algorithm for motion estimation into the iterative NLINV reconstruction (40). Practical applications range from movements of the knee (41) and temporomandibular joint (42) to studies of speaking (43) and swallowing processes (44,45). Further work includes access to myocardial strain, the separation of water and fat contributions, applications to moving table acquisitions (46) and extensions to model-based reconstructions for mapping T2 (47), T1 (48) and T2* relaxation times (49).

Real-time cardiac MRI using NLINV

Real-time cardiovascular MRI acquisitions based on undersampled radial gradient-echo sequences may be performed on existing MRI systems without the need for hardware modification and regardless of field strength. For cardiac function, the method offers the choice of two different contrast modes, i.e., spin-density or T1 contrast (depending on flip angle) using spoiled FLASH (6,7) or SSFP (T2-like) contrast using fully balanced gradients that lead to a zero gradient moment (zero phase) for each repetition time (TR) and a symmetric echo at TE = TR/2 (50). Because the NLINV reconstruction represents a nonlinear version of parallel imaging, all applications benefit from the use of optimized array coils with a large number of spatially complementary elements.

Details of experimental parameters for real-time cardiac MRI are summarized in *Table 1*. The acquisitions result in serial images with a nominal in-plane resolution ranging

from 1.2 to 1.8 mm and total imaging times (single frame) from 31 to 41 ms. All real-time MRI studies are performed during free breathing and without ECG gating, typically for about 15 s to cover a sufficiently large number of consecutive heartbeats. MRI-compatible ECG signals are still recorded to provide image time stamps relative to the last R wave in order to facilitate the post-acquisition evaluation of functional parameters by conventional software.

Real-time phase-contrast flow MRI using NLINV

Real-time MRI of through-plane flow is based on established phase-contrast principles and the use of velocity-encoding gradients (51). For this purpose, radial FLASH sequences with a motion-compensated slice-selective gradient are combined with a bipolar gradient in slice direction, which for spins flowing with constant velocity perpendicular to the imaging plane results in a net phase proportional to the velocity. Practical advantages are observed for sequential versions where bipolar flow-encoding gradients are applied in every other image (52,53). The experimental parameters for real-time phase-contrast flow MRI are comparable to those used for cardiac MRI: field of view (FOV) 192×192 mm^2, in-plane resolution 1.3×1.3 mm^2, slice thickness 6 mm, TR/TE =2.86/1.93 ms, flip angle 10°, and velocity sensitivity (VENC) 200 cm s^{-1}.

Individual flow-encoded images are obtained from only seven radial spokes (20 ms acquisition time) which, relative to the Nyquist limit, corresponds to an undersampling factor of 32. This development resulted in a total acquisition time of 40 ms for a pair of differently encoded images which then are separated into two series (movies) of magnitude images and phase-contrast velocity maps. To ensure optimum temporal accuracy, the latter are obtained without temporal filtering, while magnitude images are subjected to a post-processing median filter to alleviate residual streakings.

Online NLINV reconstruction

As far as image reconstruction is concerned, online NLINV reconstruction and display of real-time images on a 1.5 T and 3 T MRI system (Symphony and TIM Trio, Siemens Healthcare, Erlangen, Germany) were accomplished by a computer equipped with two processors (CPUs, SandyBridge E5-2650, Intel, Santa Clara, CA, USA) and eight graphical processing units (GPUs, GeForce GTX TITAN, Nvidia, Santa Clara, CA, USA) which runs a highly parallelized version of the NLINV algorithm (54). This customized computer could be fully integrated into the architecture of the commercial MRI systems, where it is invisible to the user and does not need any user interference. It effectively bypasses the standard reconstruction pipeline of the MRI systems, while storing reconstructions as conventional digital imaging and communications in medicine (DICOM) images in the regular databank (49). Currently, the online reconstruction and display rate is more than 20 frames per second (fps) for real-time cardiac images and 2×8 fps for real-time phase-contrast magnitude images and flow maps, but further speed-ups are foreseeable.

Quantitative evaluations of real-time cardiovascular MRI

The clinical information to be extracted from real-time cardiovascular MRI studies comprises all conventional functional parameters including cardiac mass, ventricular volumes at end systole and diastole, ejection fraction, peak velocities, mean velocities spatially averaged over the vessel lumen, flow rates, stroke volumes, and cardiac output. To deal with the large datasets and to provide information about beat-to-beat variations as well as responses to protocols that alter the physiologic conditions, new image evaluation programs are needed to reliably analyze hundreds of images from multiple consecutive heartbeats rather than just 25-30 images from one synthetic cycle. This particularly refers to a fully automated segmentation of the myocardial walls and vessels with little or no need for manual corrections.

Current developments of dedicated software packages are based on existing platforms such as the CAIPI software (Fraunhofer MEVIS, Bremen, Germany). It is now foreseeable that advanced programs will be able to derive the information required for a separation of serial images into individual cardiac cycles from the real-time MRI movies themselves, i.e., without the need for any external ECG time stamps. Similarly, it will become possible to retrospectively synchronize the respiratory condition for sequentially acquired movies from neighboring sections, e.g., short-axis views, to achieve a complete 3D reconstruction of the dynamic heart in a 4D dataset.

Clinical applications

In a clinical scenario, the most relevant advantages of a reliable and robust real-time MRI method are the improved

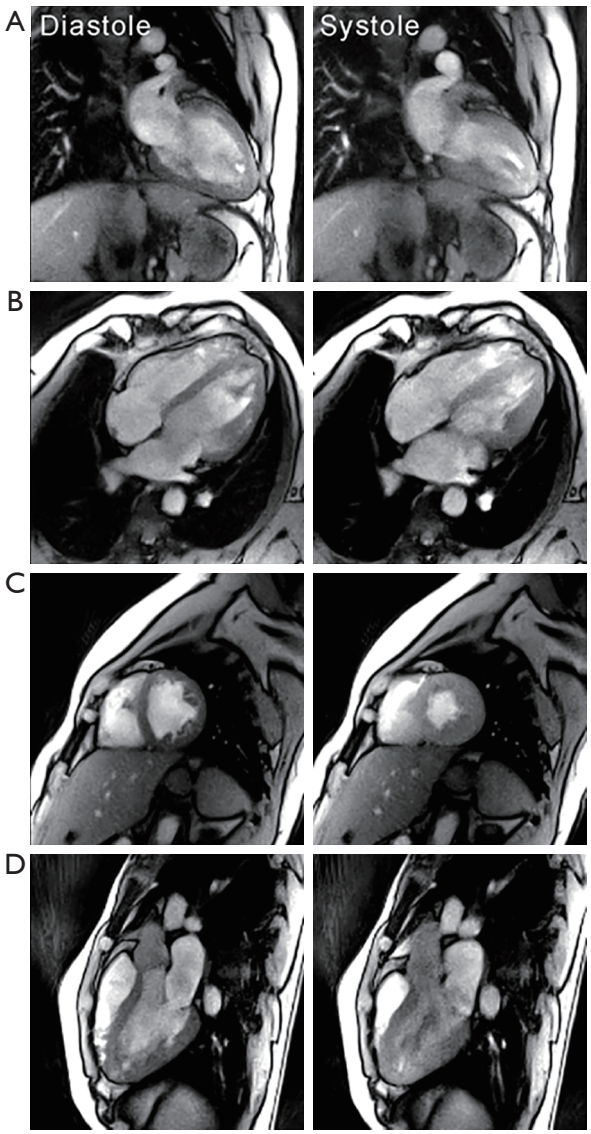

Figure 1 Real-time cardiac MRI with T1 contrast at 3 T (33 ms resolution). End-diastolic and end-systolic images of a healthy subject in (A) a 2-chamber view; (B) 4-chamber view; (C) short-axis view; and (D) 3-chamber view. Real-time MRI was performed using highly undersampled radial gradient-echo sequences and NLINV reconstruction. For experimental details see *Table 1*. MRI, magnetic resonance imaging; NLINV, nonlinear inversion.

patient compliance (e.g., no need for breathing protocols) and the extended diagnostic capabilities which arise from functional access to individual cardiac cycles. While the former increases the range of examinations to subjects with compromised respiratory control such as children or older patients and further leads to better image quality without motion sensitivity, the latter most obviously applies to patients with arrhythmias (mainly atrial fibrillation) or wall motion abnormalities. Moreover, real-time MRI allows for direct monitoring of both ventricles during ergometry in patients with ischemic or other cardiomyopathies or during stress tests in young children with congenital heart defects before and after repair. Other promising applications will be restrictive and constrictive cardiomyopathies where the ability to detect direct interactions between the ventricles adds important information. Such studies may even help in the early diagnosis of pathologies such as diastolic dysfunction. With respect to blood flow, real-time flow analyses provide information about beat-to-beat variations in flow velocity and volume simultaneously in more than one vessel. Future extensions will be MRI-guided catheterization and interventions that depend on real-time imaging with catheter tracking.

Clinical evaluations of the heart often require a comprehensive three-dimensional coverage of the myocardium. This may efficiently be accomplished using real-time MRI by sequential "multi-slice movie" acquisitions followed by the application of advanced post-processing software. For example, the acquisition part may involve 12 directly neighboring sections each with movies of 10 s duration, so that the anatomical/functional exam of the entire heart will be completed within 2 min. The processing part will require software for automatic separation of individual cardiac cycles and co-registration of individual sections in order to take breathing conditions into account. When adding adenosine stress as well as late enhancement studies and considering their inherent waiting periods, it is foreseeable to reduce the total duration of a cardiac exam to about 20 min.

Real-time MRI of cardiac function

Healthy subjects

Figure 1 shows selected frames from T1-weighted real-time MRI movies of the heart of a healthy subject at 3 T. While the choice of spatial and temporal resolution is user dependent, high-quality images may be obtained with only 15 radial spokes and 1.6 mm in-plane resolution within an image acquisition time of 33.3 ms (yielding 30 fps). In contrast to cine acquisitions with Cartesian phase-encoding gradients, there is no need for a large FOV along the phase-encoding direction of the image. This is because radial

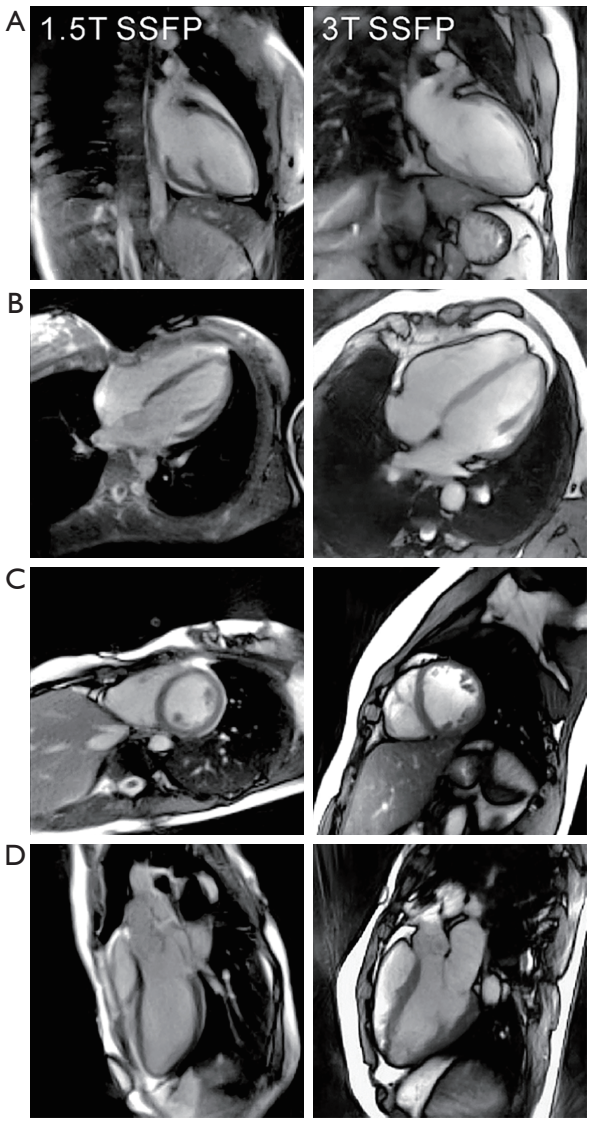

Figure 2 Real-time cardiac MRI with SSFP contrast at 1.5 T (41 ms) and 3 T (31 ms). End-diastolic images of a healthy subject in (A) a 2-chamber view; (B) 4-chamber view; (C) short-axis view; and (D) 3-chamber view. Other parameters as in *Figure 1*. MRI, magnetic resonance imaging; SSFP, steady-state free precession.

trajectories with frequency-encoding gradients only and standard oversampling do not suffer from aliasing when using relatively small FOVs of, for example, 256×256 mm^2. Typically, flip angles of 8° to 10° result in T1-weighted images where bright blood signals contain information about inflow phenomena (e.g., turbulent flow patterns) (6,7). The minimum gradient-echo times (TE) achieved here (see *Table 1*) roughly correspond to opposed-phase conditions for water and fat protons at a field strength of 3 T (intravoxel cancellation of respective signal contributions) and in-phase conditions at 1.5 and 7 T (constructive overlap).

So far, most clinical cardiac MRI examinations are performed with SSFP contrast at a field strength of 1.5 T. *Figure 2* compares selected end-diastolic frames from real-time MRI movies obtained with SSFP contrast at 1.5 T and 3 T. Equivalent to respective cine MRI studies, SSFP conditions with fully balanced gradients result in more homogeneous representations of the blood pool and thereby maximize the contrast between blood and myocardium (50). In fact, at 3 T the SSFP version with only 11 spokes per image yields even better SNR than the comparable FLASH version with T1 contrast and 15 spokes (compare *Figure 1*). On the other hand, the SSFP images are prone to residual "banding" artifacts which are caused by magnetic field inhomogeneities or susceptibility differences in the thoracic and abdominal regions (not visible in the example shown in *Figure 2*). This problem is much reduced at the lower field of 1.5 T where high-quality real-time images were obtained with 15 spokes within 41 ms. Noteworthy, the low-field results shown here stem from an older MRI system, while state-of-the-art gradient systems and multi-element receive coils will further improve the image quality and speed of respective applications. In general, it seems advisable to perform real-time cardiac MRI at 1.5 T with fully balanced sequence versions and SSFP contrast and at higher fields with FLASH sequences and T1 contrast.

First results obtained for T1-weighted real-time MRI of the heart at 7 T (MAGNETOM, Siemens Healthcare, Erlangen, Germany) are summarized in *Figure 3* using a specially developed transmit/receive coil array with 16 elements (55,56). With recent improvements in coil design (57,58), these ultrahigh fields offer the chance to further increase the spatial resolution of real-time cardiac MRI.

Preliminary patient studies

Clinical examples are presented in *Figures 4* and *5* for two patients with supraventricular arrhythmias and abnormal wall motion, respectively. They demonstrate the advantageous properties of real-time MRI recordings which are not affected by respiratory motions or irregular heartbeats. For the patient in *Figure 4*, conventional cine SSFP MRI failed to properly sort the data according to the ECG because of frequent aperiodic heart motions. The resulting inconsistencies in the MRI datasets inevitably lead to image distortions. In contrast, real-time MRI successfully

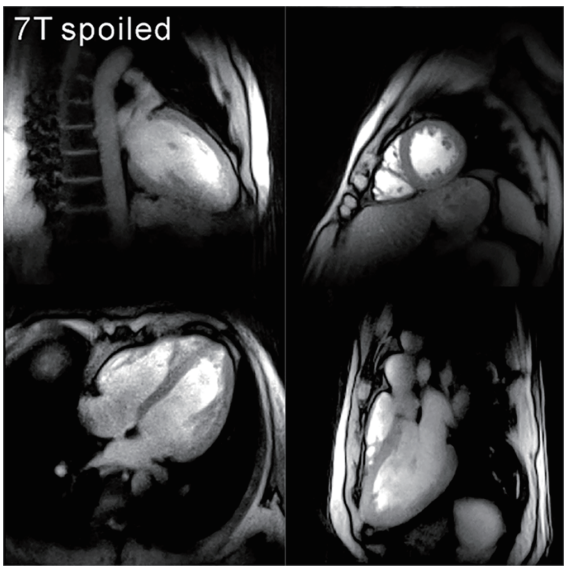

Figure 3 Real-time cardiac MRI with T1 contrast at 7 T (33 ms). End-diastolic images of a healthy subject in a 2-chamber view, 4-chamber view, short-axis view, and 3-chamber view. Other parameters as in *Figure 1*. MRI, magnetic resonance imaging.

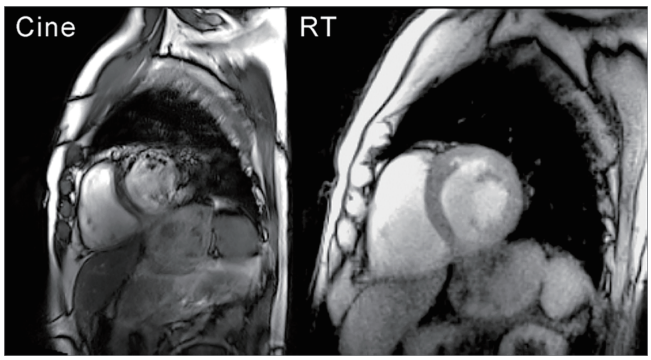

Figure 4 Cine SSFP MRI *vs.* real-time MRI with T1 contrast (3 T, 33 ms) of a 79-year-old male patient with supraventricular arrhythmias. While end-diastolic SSFP cine images suffer from distortions due to irregular heartbeats, real-time MRI resolves myocardial motions without image degradation (see *Figures 6* and 7). MRI, magnetic resonance imaging; SSFP, steady-state free precession.

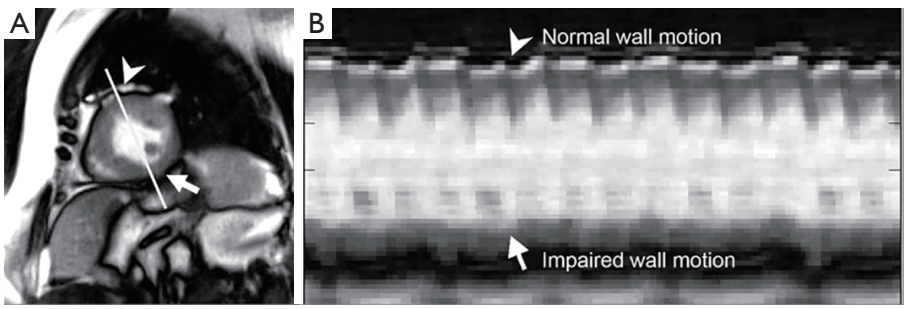

Figure 5 Real-time cardiac MRI with SSFP contrast (1.5 T, 41 ms) of a patient with abnormal motions of the inferior and infero-lateral segments of the left-ventricular wall after myocardial infaction. (A) End-systolic image from a corresponding movie (see *Figure 8*); (B) temporal intensity profiles along the indicated reference line demonstrate impaired wall motion (arrows) in comparison to normal contractions (arrow heads). The diagram covers a period of 14 cardiac cycles (295 images =11.8 s). MRI, magnetic resonance imaging; SSFP, steady-state free precession.

resolves arbitrary myocardial motions in individual heartbeats with no induced distortions (compare *Figures 6* and 7).

Figure 5 shows a patient with abnormal motion of the inferior and infero-lateral segments of the left-ventricular myocardial wall due to prior infarction. As recently proposed ["1D arrhythmia plot" (50)] the characterization of irregular events or movements may conveniently be depicted by evaluating one-dimensional temporal intensity profiles along a reference line for a series of consecutive real-time images, similar to the M-mode known from echocardiography. For the patient in *Figure 5* the chosen profile directly compares regular contractility in the anterior wall of the myocardium with the impaired performance of the damaged tissue in the inferior wall segments. The compromised wall thickening and contraction can also be seen in *Figure 8*. In general, quantitative analyses of wall motion based on the 17-segment AHA model and Simpson's rule yield information about global myocardial function, ventricular volume and ventricular mass. With conventional cine MRI this is accomplished for a stack of parallel sections, each being the result of 10-12 heartbeats. Extending this

Figure 6 Cine cardiac MRI with SSFP contrast (3 T) of a patient with supraventricular arrhythmias (59). For details see *Figure 4*. MRI, magnetic resonance imaging; SSFP, steady-state free precession. Available online: http://www.asvide.com/articles/301

Figure 7 Real-time cardiac MRI with T1 contrast (3 T, 33 ms) of a patient with supraventricular arrhythmias (same as in *Figure 6*) (60). MRI, magnetic resonance imaging. Available online: http://www.asvide.com/articles/302

approach, real-time MRI offers a quantitative assessment of every single cardiac cycle which promises more accurate insights into myocardial wall motion. This especially applies to subjects with arrhythmias or higher heart rate or during exercise. Similar arguments hold true for real-time MRI studies with myocardial tagging and corresponding strain analyses. Such examinations provide relevant clinical parameters for single heartbeats as well as their beat-to-beat variation compared to mean data from multiple cycles.

Figure 9 demonstrates results of a patient with diastolic dysfunction during a Valsalva maneuver as a stress test. The clinical history of the patient comprises arterial hypertension and coronary artery disease with operative revascularization (left-ventricular ejection fraction 68%). In order to directly monitor physiologic alterations in response

Figure 8 Real-time cardiac MRI with SSFP contrast (1.5 T, 40 ms) of a patient with abnormal motion of the left-ventricular myocardial wall (61). For details see *Figure 5*. MRI, magnetic resonance imaging; SSFP, steady-state free precession. Available online: Available online: http://www.asvide.com/articles/303

to induced pressure changes, T1-weighted real-time images at 33 ms resolution (short-axis view) were acquired during normal breathing (10 s), increased intrathoracic pressure (10 s) and recovery (normal breathing for 20 s). Again, the direction and amount of the myocardial motion during prolonged pressure increase is clearly visualized in the temporal intensity profiles of two orthogonal reference lines cutting through the left-ventricular myocardial wall. The effect is also well demonstrated in *Figure 10* which comprises three phases: (I) normal breathing with normal contraction of the septum; (II) Valsalva maneuver with reduced right- and left-ventricular volumes; and (III) D-shaped contraction pattern of the septum immediately after pressure release due to the overshoot of blood flowing into the right heart. Septal contraction normalizes after several beats as in healthy subjects. These studies represent unique opportunities only offered by real-time MRI. They may lead to new insights and the development of novel tests for diagnostic imaging of the still asymptomatic heart.

Real-time phase-contrast MRI of cardiac blood flow

Healthy subjects

Figure 11 summarizes magnitude images and phase-contrast velocity maps of the ascending and descending aorta, superior vena cava, pulmonary trunk and pulmonary arteries of a healthy subject during systole. They are selected from respective real-time MRI movies (40 ms resolution)

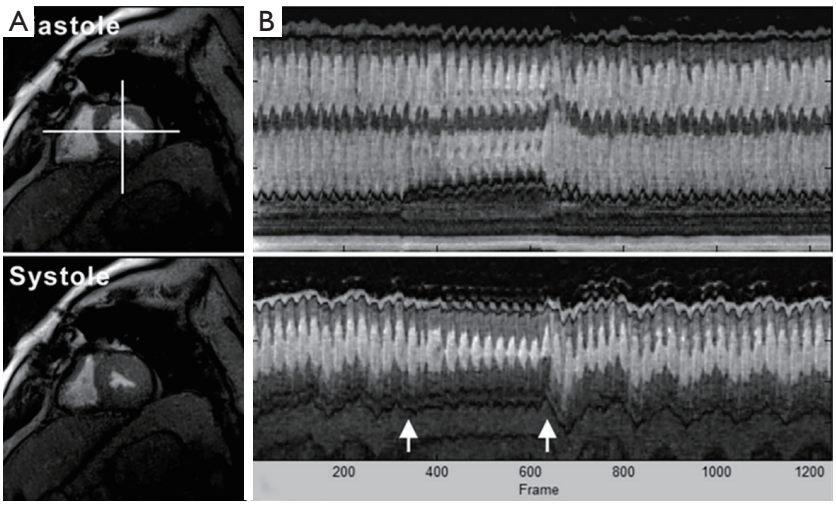

Figure 9 Real-time cardiac MRI with T1 contrast (3 T, 33 ms) of a patient with diastolic dysfunction during Valsalva maneuver, i.e., increased intrathoracic pressure. (A) End-diastolic and end-systolic images from a corresponding movie (see *Figure 10*); (B) temporal intensity profiles (40 s, top = horizontal reference, bottom = vertical reference) demonstrate reduced systolic and diastolic myocardial movements as well as alterations of wall thickening during Valsalva maneuver (arrows). MRI, magnetic resonance imaging.

Figure 10 Real-time cardiac MRI with T1 contrast (3 T, 33 ms) of a patient with diastolic dysfunction during Valsalva maneuver (62). For details see *Figure 9*. MRI, magnetic resonance imaging. Available online: http://www.asvide.com/articles/304

and represent situations with strong cardiac outflow. The achievable image quality supports a reliable segmentation of vessels which in diastolic phases is even better than usually obtainable by cine MRI recordings [e.g., see (53)]. Residual streaking artifacts in phase-contrast maps may appear during systole because reconstructions from extremely undersampled data are mainly affected by rapid intensity changes with high spatial frequencies and the lack of a temporal filter. However, for the same reason these artifacts occur outside the vessel lumen, i.e., the area of interest for quantitative flow evaluations. Real-time phase-contrast flow MRI is thus possible for all major heart vessels.

A transient problem for the clinical use of real-time cardiovascular MRI is the automatic and reliable segmentation of myocardial structures and vessels from hundreds of images without manual interference. For real-time flow studies *Figure 12* shows a promising strategy based on recent developments of the CAIPI software (Fraunhofer MEVIS, Bremen, Germany) (63). Robust automated segmentation of the ascending aorta is followed by a definition of blood flow velocities and a subsequent visualization of peak velocities, mean velocities averaged across the vessel lumen and minimum velocities (overlayed in *Figure 12*). The real-time evolution for a consecutive series of 17 heartbeats directly demonstrates the influence of respiration which leads to higher velocities during inspiration (i.e., reduced intrathoracic pressure) than during exspiration. Corresponding analyses of temporal velocity profiles for the subject and vessels shown in *Figure 11* are summarized in *Figure 13* depicting the data of only a single selected cardiac cycle.

Subsequent functional analyses comprise stroke volumes and flow rates for each individual heartbeat. Such information may uniquely be exploited for a detailed characterization of the immediate physiologic responses to stress or exercise. For example, *Figure 14* compares simultaneous alterations of the mean blood flow velocity and resulting stroke volume in the ascending aorta with adjustments of the heart rate before, during and after a Valsalva maneuver. This flow study

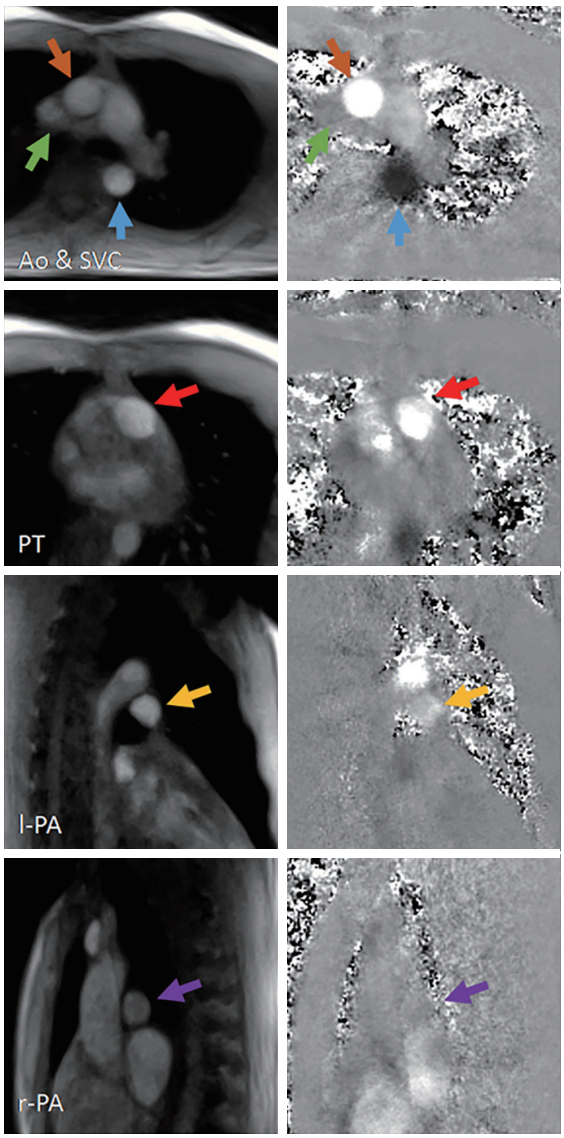

Figure 11 Real-time phase-contrast flow MRI (3 T, 40 ms): magnitude images and phase-contrast maps (20 ms each) of a healthy subject during systole for the ascending and descending aorta (Ao), superior vena cava (SVC), pulmonary trunk (PT), left (l-PA) and right pulmonary artery (r-PA). Real-time phase-contrast flow MRI was performed using sequential acquisitions of highly undersampled radial gradient-echo images with and without a bipolar velocity-encoding gradient and phase-sensitive NLINV reconstructions without temporal filter. MRI, magnetic resonance imaging; NLINV, regularized nonlinear inversion.

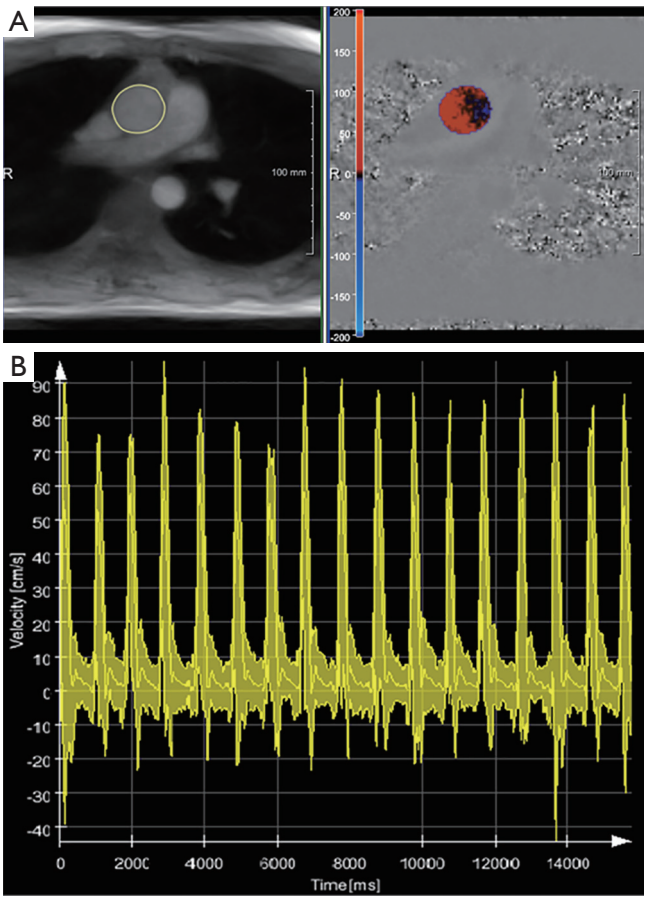

Figure 12 Real-time phase-contrast flow MRI (3 T, 40 ms): Quantitative evaluations for the ascending aorta of a healthy subject using CAIPI software. (A) End-systolic magnitude image and phase-contrast map with segmented ascending aorta and color-coded flow velocities, respectively; (B) the overlay of peak flow velocity, mean velocity averaged over the lumen of the aorta and minimum velocity as a function of time for 17 consecutive heartbeats demonstrates the influence of respiration. MRI, magnetic resonance imaging.

of a healthy subject employed a similar protocol as used for real-time cardiac MRI in *Figure 9*. To control for the target pressure increase of 40 mmHg during the 10 s maneuver, the oropharyngeal pressure was measured (GMSD 2 BR, Greisinger electronic GmbH, Regenstauf, Germany) and shown to the subject in real time through a visual feedback system (projector, mirror).

During continuously elevated intrathoracic pressure the aortic blood flow as given by the stroke volume becomes drastically reduced. This is a consequence of both a reduced venous inflow and a lower cardiac outflow due to a decreased velocity and smaller (compressed) aortic lumen during the maneuver. To compensate for the lower

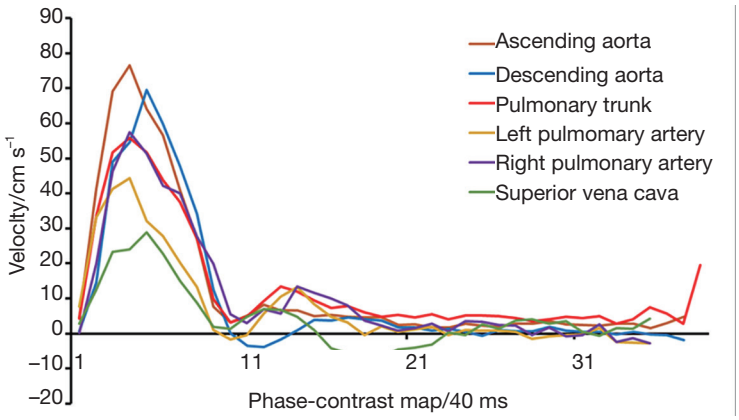

Figure 13 Real-time phase-contrast flow MRI (3 T, 40 ms) of major heart vessels for a single cardiac cycle (same subject as in *Figure 11*). The curves represent mean blood flow velocities averaged across the respective vessel lumen for the ascending and descending aorta, pulmonary trunk, left and right pulmonary artery, and superior vena cava. MRI, magnetic resonance imaging.

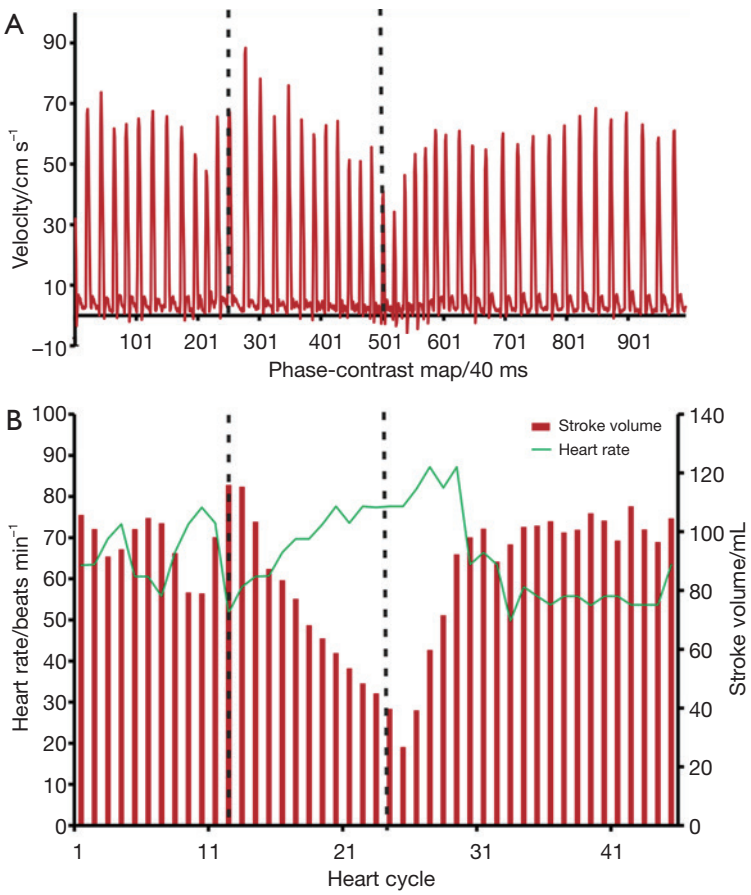

Figure 14 Real-time phase-contrast flow MRI (3 T, 40 ms) of the ascending aorta of a healthy subject during Valsalva maneuver comprising 10 s of normal breathing, 10 s of increased intrathoracic pressure (broken lines) and 20 s of normal breathing. (A) Mean blood flow velocity averaged across vessel lumen as a function of phase-contrast map; (B) stroke volume as a function of cardiac cycle. MRI, magnetic resonance imaging.

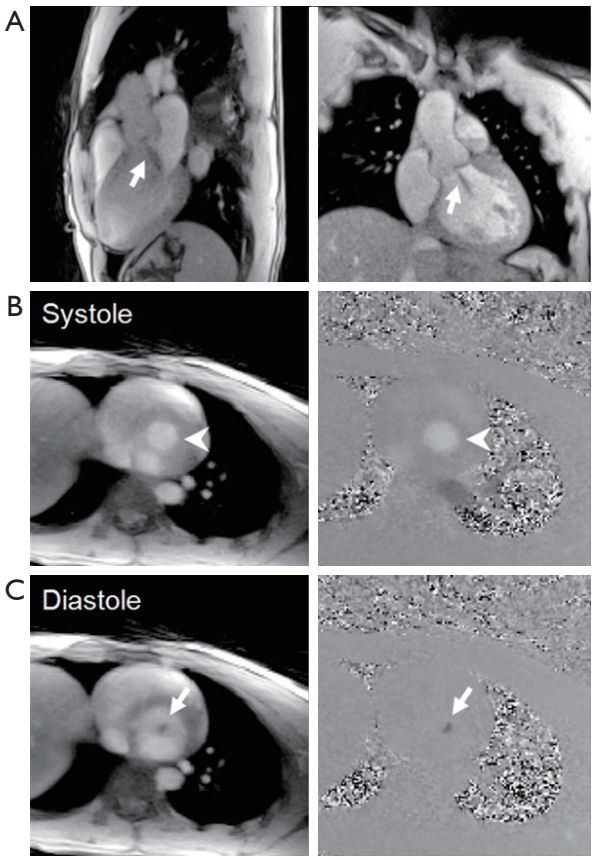

Figure 15 (A) Real-time cardiac MRI (3 T, 33 ms) and (B,C) real-time phase-contrast flow MRI (3 T, 37 ms) of a 25-year-old male patient with mild aortic insufficiency. (A) Selected images in a 3-chamber and coronal view demonstrate aortic regurgitation (arrows), see *Figures 16* and *17*; (B) During systole, real-time magnitude images and phase-contrast maps reveal normal cardiac outflow at about the level of the aortic valve (arrow heads); whereas (C) diastolic phases are affected by pronounced regurgitation from the aorta back into the left ventricle (arrows), see *Figures 18* and *19*. MRI, magnetic resonance imaging.

cardiac output, the heart rate is increased. After return to normal breathing, the cardiac performance rapidly recovers to baseline levels. In general, however, these serial functional observations are expected to change for specific pathologic conditions, which is why the Valsalva maneuver has previously been proposed as a physiologic stress test and diagnostic indicator for cardiovascular disease (64,65). Real-time phase-contrast flow MRI may now further explore this potential by monitoring the immediate hemodynamic and physiologic responses to stress and exercise.

Figure 16 Real-time cardiac MRI with T1 contrast (3 T, 33 ms) of a patient with mild aortic insufficiency: 3-chamber view (66). For details see *Figure 14*. MRI, magnetic resonance imaging. Available online: http://www.asvide.com/articles/305

Figure 17 Real-time cardiac MRI with T1 contrast (3 T, 33 ms) of a patient with mild aortic insufficiency: coronal view (same as in *Figure 16*) (67). MRI, magnetic resonance imaging. Available online: http://www.asvide.com/articles/306

Preliminary patient studies

Figure 15 presents real-time cardiovascular MRI results for a 25-year-old male patient suffering from mild aortic insufficiency. Because T1-weighted real-time cardiac MRI provides contrast within the blood pool that reflects through-plane flow (i.e., signal increase due to reduced saturation) as well as turbulent phenomena (i.e., signal decrease due to dephasing), respective movies (see *Figures 16* and *17*) directly unravel the occurrence of back flow into the left ventricle (*Figure 15A*).

Real-time phase-contrast flow MRI in a perpendicular section at about the level of the aortic valve further demonstrates and quantifies this regurgitation. During systole (*Figure 15B*), the blood is represented as bright

Figure 18 Real-time phase-contrast flow MRI (3 T, 37 ms) of a patient with mild aortic insufficiency: magnitude images (same as in *Figure 16*) (68). MRI, magnetic resonance imaging. Available online: http://www.asvide.com/articles/307

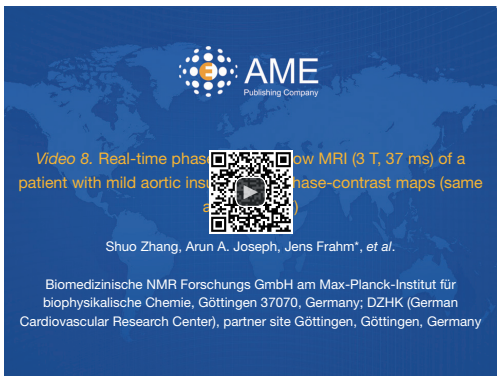

Figure 19 Real-time phase-contrast flow MRI (3 T, 37 ms) of a patient with mild aortic insufficiency: phase-contrast maps (same as in *Figure 16*) (69). MRI, magnetic resonance imaging. Available online: http://www.asvide.com/articles/308

signal in both magnitude images (inflow) and phase-contrast maps (high velocities) indicating cardiac outflow from the left ventricle into the ascending aorta. On the other hand, during diastolic phases (*Figure 15C*), the magnitude images are characterized by a focal signal void (dephasing), while the corresponding phase-contrast maps reveal reversed blood flow back into the ventricle. These differences are also well visualized in *Figures 18* and *19*.

Challenges and perspectives

Although real-time cardiovascular MRI represents a most challenging field of application for ultrafast dynamic imaging, examinations of myocardial anatomy, function, and flow during free breathing and independent of ECG synchronization promise significant benefits which range from improved patient compliance and extended diagnostic capabilities to temporal (economic) efficiency. Despite their preliminary character the present results confirm that real-time cardiovascular MRI will generally reach diagnostic quality, while already being superior for patients with irregular heartbeats.

At this stage a certain difficulty for achieving clinical acceptance appears to be the absence of a true gold standard for real-time cardiac performance. This lack hampers necessary "validation" studies and complicates comparisons of real-time MRI to cine MRI methods or ultrasound techniques none of which offer the ground truth. For example, the previous observation of a 10% lower ejection fraction (averaged across patients) in real-time *vs*. cine MRI examinations (53) remains difficult to interpret as both methods possess systematic differences in terms of image acquisition technique and physiologic coverage.

Other obstacles for a rapid translation of real-time MRI into the clinical arena are the high computational demand of NLINV reconstructions and the urgent need for advanced post-processing tools that offer reliable tissue segmentation for large image series with minimal user interference. While considerable progress has already been made with respect to the former problem, the current lack of fast and reliable software for the quantitative analysis of real-time MRI datasets has to be overcome in order to enable widespread clinical application. A move to routine real-time cardiac MRI may therefore take longer than its mere technical implementation and will further require a sufficient base of evidence from extended clinical trials.

Finally, ongoing developments aim to extend the current methods for cardiac function and flow toward a more comprehensive MRI evaluation of the heart in real time. Such future examinations should not only include a full three-dimensional coverage of the heart with access to tissue perfusion and viability, but also reduce the overall examination time to less than 20 min.

Acknowledgements

Financial support by the DZHK (German Centre for Cardiovascular Research) and BMBF (German Ministry of Education and Research) as well as by the Max-Planck-Gesellschaft and Fraunhofer Gesellschaft is gratefully acknowledged. We thank Thoralf Niendorf, Lukas Winter and Andreas Graessl, Ultra-High Field Facility

at the Max Delbrück Center for Molecular Medicine, Berlin-Buch, Germany, for collaborative research at 7 T, Teodora Chitiboi, Markus Huellebrand and Lennart Tautz, Fraunhofer MEVIS, Bremen, Germany, for the devopment of CAIPI software, and Jan M. Sohns, Martin Fasshauer, and Johannes T. Kowallick, Universitätsmedizin Göttingen, Germany, for clinical collaborations.

Disclosure: The authors declare no conflict of interest.

References

1. Thom T, Haase N, Rosamond W, Howard VJ, Rumsfeld J, Manolio T, Zheng ZJ, Flegal K, O'Donnell C, Kittner S, Lloyd-Jones D, Goff DC Jr, Hong Y, Adams R, Friday G, Furie K, Gorelick P, Kissela B, Marler J, Meigs J, Roger V, Sidney S, Sorlie P, Steinberger J, Wasserthiel-Smoller S, Wilson M, Wolf P; American Heart Association Statistics Committee and Stroke Statistics Subcommittee. Heart disease and stroke statistics--2006 update: a report from the American Heart Association Statistics Committee and Stroke Statistics Subcommittee. Circulation 2006;113:e85-151.
2. Ishida M, Kato S, Sakuma H. Cardiac MRI in ischemic heart disease. Circ J 2009;73:1577-88.
3. Steinmetz M, Preuss HC, Lotz J. Non-invasive imaging for congenital heart disease – Recent progress in cardiac MRI. J Clin Exp Cardiolog 2012;S8:008.
4. White RD, Patel MR, Abbara S, Bluemke DA, Herfkens RJ, Picard M, Shaw LJ, Silver M, Stillman AE, Udelson J; American College of Radiology; American College of Cardiology Foundation. 2013 ACCF/ACR/ASE/ASNC/SCCT/SCMR appropriate utilization of cardiovascular imaging in heart failure: an executive summary: a joint report of the ACR Appropriateness Criteria ® Committee and the ACCF Appropriate Use Criteria Task Force. J Am Coll Radiol 2013;10:493-500.
5. Achenbach S, Barkhausen J, Beer M, Beerbaum P, Dill T, Eichhorn J, Fratz S, Gutberlet M, Hoffmann M, Huber A, Hunold P, Klein C, Krombach G, Kreitner KF, Kühne T, Lotz J, Maintz D, Mahrholdt H, Merkle N, Messroghli D, Miller S, Paetsch I, Radke P, Steen H, Thiele H, Sarikouch S, Fischbach R. Consensus recommendations of the German Radiology Society (DRG), the German Cardiac Society (DGK) and the German Society for Pediatric Cardiology (DGPK) on the use of cardiac imaging with computed tomography and magnetic resonance imaging. Rofo 2012;184:345-68.
6. Uecker M, Zhang S, Voit D, Karaus A, Merboldt KD, Frahm J. Real-time MRI at a resolution of 20 ms. NMR Biomed 2010;23:986-94.
7. Zhang S, Uecker M, Voit D, Merboldt KD, Frahm J. Real-time cardiovascular magnetic resonance at high temporal resolution: radial FLASH with nonlinear inverse reconstruction. J Cardiovasc Magn Reson 2010;12:39.
8. Mansfield P. Real-time echo-planar imaging by NMR. Br Med Bull 1984;40:187-90.
9. Haase A, Frahm J, Matthaei D, Hänicke W, Merboldt KD. FLASH imaging: rapid NMR imaging using low flip-angle pulses. 1986. J Magn Reson 2011;213:533-41.
10. Frahm J, Haase A, Matthaei D. Rapid NMR imaging of dynamic processes using the FLASH technique. Magn Reson Med 1986;3:321-7.
11. Hennig J, Nauerth A, Friedburg H. RARE imaging: a fast imaging method for clinical MR. Magn Reson Med 1986;3:823-33.
12. Oppelt A, Graumann R, Barfuss H, Fischer H, Hartl W, Schajor W. FISP: a new fast MRI sequence. Electromedica 1986;54:15-8.
13. Scheffler K, Lehnhardt S. Principles and applications of balanced SSFP techniques.Eur Radiol 2003;13:2409-18.
14. Sodickson DK, Manning WJ. Simultaneous acquisition of spatial harmonics (SMASH): fast imaging with radiofrequency coil arrays. Magn Reson Med 1997;38:591-603.
15. Pruessmann KP, Weiger M, Scheidegger MB, Boesiger P. SENSE: sensitivity encoding for fast MRI. Magn Reson Med 1999;42:952-62.
16. Griswold MA, Jakob PM, Heidemann RM, Nittka M, Jellus V, Wang J, Kiefer B, Haase A. Generalized autocalibrating partially parallel acquisitions (GRAPPA). Magn Reson Med 2002;47:1202-10.
17. Ahn CB, Kim JH, Cho ZH. High-speed spiral-scan echo planar NMR imaging-I. IEEE Trans Med Imaging 1986;5:2-7.
18. Meyer CH, Hu BS, Nishimura DG, Macovski A. Fast spiral coronary artery imaging. Magn Reson Med 1992;28:202-13.
19. Nayak KS, Hargreaves BA, Hu BS, Nishimura DG, Pauly JM, Meyer CH. Spiral balanced steady-state free precession cardiac imaging. Magn Reson Med 2005;53:1468-73.
20. Scheffler K, Hennig J. Reduced circular field-of-view imaging. Magn Reson Med 1998;40:474-80.
21. Peters DC, Korosec FR, Grist TM, Block WF, Holden JE, Vigen KK, Mistretta CA. Undersampled projection

reconstruction applied to MR angiography. Magn Reson Med 2000;43:91-101.
22. Rasche V, de Boer RW, Holz D, Proksa R. Continuous radial data acquisition for dynamic MRI. Magn Reson Med 1995;34:754-61.
23. Block KT, Uecker M, Frahm J. Undersampled radial MRI with multiple coils. Iterative image reconstruction using a total variation constraint. Magn Reson Med 2007;57:1086-98.
24. Zhang S, Block KT, Frahm J. Magnetic resonance imaging in real time: advances using radial FLASH. J Magn Reson Imaging 2010;31:101-9.
25. Bauer RW, Radtke I, Block KT, Larson MC, Kerl JM, Hammerstingl R, Graf TG, Vogl TJ, Zhang S. True real-time cardiac MRI in free breathing without ECG synchronization using a novel sequence with radial k-space sampling and balanced SSFP contrast mode. Int J Cardiovasc Imaging 2013;29:1059-67.
26. Jakob PM, Griswold MA, Edelman RR, Manning WJ, Sodickson DK. Accelerated cardiac imaging using the SMASH technique. J Cardiovasc Magn Reson 1999;1:153-7.
27. Pruessmann KP, Weiger M, Boesiger P. Sensitivity encoded cardiac MRI. J Cardiovasc Magn Reson 2001;3:1-9.
28. Kühl HP, Spuentrup E, Wall A, Franke A, Schröder J, Heussen N, Hanrath P, Günther RW, Buecker A. Assessment of myocardial function with interactive non-breath-hold real-time MR imaging: comparison with echocardiography and breath-hold Cine MR imaging. Radiology 2004;231:198-207.
29. Winkelmann S, Schaeffter T, Koehler T, Eggers H, Doessel O. An optimal radial profile order based on the Golden Ratio for time-resolved MRI. IEEE Trans Med Imaging 2007;26:68-76.
30. Peters DC, Ennis DB, Rohatgi P, Syed MA, McVeigh ER, Arai AE. 3D breath-held cardiac function with projection reconstruction in steady state free precession validated using 2D cine MRI. J Magn Reson Imaging 2004;20:411-6.
31. Arunachalam A, Samsonov A, Block WF. Self-calibrated GRAPPA method for 2D and 3D radial data. Magn Reson Med 2007;57:931-8.
32. Liu J, Wieben O, Jung Y, Samsonov AA, Reeder SB, Block WF. Single breathhold cardiac CINE imaging with multi-echo three-dimensional hybrid radial SSFP acquisition. J Magn Reson Imaging 2010;32:434-40.
33. Liu J, Spincemaille P, Codella NC, Nguyen TD, Prince MR, Wang Y. Respiratory and cardiac self-gated free-breathing cardiac CINE imaging with multiecho 3D hybrid radial SSFP acquisition. Magn Reson Med 2010;63:1230-7.
34. Tsao J, Kozerke S, Boesiger P, Pruessmann KP. Optimizing spatiotemporal sampling for k-t BLAST and k-t SENSE: application to high-resolution real-time cardiac steady-state free precession. Magn Reson Med 2005;53:1372-82.
35. Feng L, Srichai MB, Lim RP, Harrison A, King W, Adluru G, Dibella EV, Sodickson DK, Otazo R, Kim D. Highly accelerated real-time cardiac cine MRI using k-t SPARSE-SENSE. Magn Reson Med 2013;70:64-74.
36. Seiberlich N, Ehses P, Duerk J, Gilkeson R, Griswold M. Improved radial GRAPPA calibration for real-time free-breathing cardiac imaging. Magn Reson Med 2011;65:492-505.
37. Uecker M, Hohage T, Block KT, Frahm J. Image reconstruction by regularized nonlinear inversion--joint estimation of coil sensitivities and image content. Magn Reson Med 2008;60:674-82.
38. Uecker M, Zhang S, Frahm J. Nonlinear inverse reconstruction for real-time MRI of the human heart using undersampled radial FLASH. Magn Reson Med 2010;63:1456-62.
39. Frahm J, Schätz S, Untenberger M, Zhang S, Voit V, Merboldt KD, Sohns JM, Lotz J, Uecker M. On the temporal fidelity of nonlinear inverse reconstructions for real-time MRI – The motion challenge. The Open Med Imaging J 2014;8:1-7.
40. Li H, Haltmeier M, Zhang S, Frahm J, Munk A. Aggregated motion estimation for real-time MRI reconstruction. Magn Reson Med 2014;72:1039-48.
41. Lin CC, Zhang S, Frahm J, Lu TW, Hsu CY, Shih TF. A slice-to-volume registration method based on real-time magnetic resonance imaging for measuring three-dimensional kinematics of the knee. Med Phys 2013;40:102302.
42. Zhang S, Gersdorff N, Frahm J. Real-time magnetic resonance imaging of temporomandibular joint dynamics. The Open Med Imaging J 2011;5:1-9.
43. Niebergall A, Zhang S, Kunay E, Keydana G, Job M, Uecker M, Frahm J. Real-time MRI of speaking at a resolution of 33 ms: undersampled radial FLASH with nonlinear inverse reconstruction. Magn Reson Med 2013;69:477-85.
44. Zhang S, Olthoff A, Frahm J. Real-time magnetic resonance imaging of normal swallowing. J Magn Reson Imaging 2012;35:1372-9.
45. Olthoff A, Zhang S, Schweizer R, Frahm J. On the

physiology of normal swallowing as revealed by magnetic resonance imaging in real time. Gastroenterol Res Pract 2014;2014:493174.
46. Zenge MO, Uecker M, Mattauch G, Frahm J. Continuous table movement MRI in a single breath-hold: Highly undersampled radial acquisitions with nonlinear iterative reconstruction and joint coil estimation. Proc Intl Soc Mag Reson Med 2012, May 5-11, Melbourne, Australia.
47. Sumpf TJ, Uecker M, Boretius S, Frahm J. Model-based nonlinear inverse reconstruction for T2 mapping using highly undersampled spin-echo MRI. J Magn Reson Imaging 2011;34:420-8.
48. Zhang S, Uecker M, Frahm J. T1 mapping in real time: Single inversion-recovery radial FLASH with nonlinear inverse reconstruction. Annual Meeting ISMRM, Salt Lake City 2013, In Proc Intl Soc Mag Reson Med 2013;21:3700.
49. Uecker M, Zhang S, Voit D, Merboldt KD, Frahm J. Real-time MRI: recent advances using radial FLASH. Imaging Med 2012;4:461-76.
50. Voit D, Zhang S, Unterberg-Buchwald C, Sohns JM, Lotz J, Frahm J. Real-time cardiovascular magnetic resonance at 1.5 T using balanced SSFP and 40 ms resolution. J Cardiovasc Magn Reson 2013;15:79.
51. Lotz J, Meier C, Leppert A, Galanski M. Cardiovascular flow measurement with phase-contrast MR imaging: basic facts and implementation. Radiographics 2002;22:651-71.
52. Joseph AA, Merboldt KD, Voit D, Zhang S, Uecker M, Lotz J, Frahm J. Real-time phase-contrast MRI of cardiovascular blood flow using undersampled radial fast low-angle shot and nonlinear inverse reconstruction. NMR Biomed 2012;25:917-24.
53. Joseph A, Kowallick JT, Merboldt KD, Voit D, Schaetz S, Zhang S, Sohns JM, Lotz J, Frahm J. Real-time flow MRI of the aorta at a resolution of 40 msec. J Magn Reson Imaging 2014;40:206-13.
54. Schätz S, Uecker M. A multi-GPU programming library for real-time applications. In: Algorithms and Architectures for Parallel Processing (Springer). Lect Notes Comp Sci 2012;7439:114-28.
55. Thalhammer C, Renz W, Winter L, Hezel F, Rieger J, Pfeiffer H, Graessl A, Seifert F, Hoffmann W, von Knobelsdorff-Brenkenhoff F, Tkachenko V, Schulz-Menger J, Kellman P, Niendorf T. Two-dimensional sixteen channel transmit/receive coil array for cardiac MRI at 7.0 T: design, evaluation, and application. J Magn Reson Imaging 2012;36:847-57.
56. Niendorf T, Graessl A, Thalhammer C, Dieringer MA, Kraus O, Santoro D, Fuchs K, Hezel F, Waiczies S, Ittermann B, Winter L. Progress and promises of human cardiac magnetic resonance at ultrahigh fields: a physics perspective. J Magn Reson 2013;229:208-22.
57. Winter L, Özerdem C, Hoffmann W, Santoro D, Müller A, Waiczies H, Seemann R, Graessl A, Wust P, Niendorf T. Design and evaluation of a hybrid radiofrequency applicator for magnetic resonance imaging and RF induced hyperthermia: electromagnetic field simulations up to 14.0 Tesla and proof-of-concept at 7.0 Tesla. PLoS One 2013;8:e61661.
58. Graessl A, Renz W, Hezel F, Dieringer MA, Winter L, Oezerdem C, Rieger J, Kellman P, Santoro D, Lindel TD, Frauenrath T, Pfeiffer H, Niendorf T. Modular 32-channel transceiver coil array for cardiac MRI at 7.0T. Magn Reson Med 2014;72:276-90.
59. Zhang S, Joseph AA, Voit D, Schaetz S, Merboldt KD, Unterberg-Buchwald C, Hennemuth A, Lotz J, Frahm J. Cine cardiac MRI with SSFP contrast (3 T) of a patient with supraventricular arrhythmias. Asvide 2014;1:288. Available online: http://www.asvide.com/articles/301
60. Zhang S, Joseph AA, Voit D, Schaetz S, Merboldt KD, Unterberg-Buchwald C, Hennemuth A, Lotz J, Frahm J. Real-time cardiac MRI with T1 contrast (3 T, 33 ms) of a patient with supraventricular arrhythmias (same as in Figure 6). Asvide 2014;1:289. Available online: http://www.asvide.com/articles/302
61. Zhang S, Joseph AA, Voit D, Schaetz S, Merboldt KD, Unterberg-Buchwald C, Hennemuth A, Lotz J, Frahm J. Real-time cardiac MRI with SSFP contrast (1.5 T, 40 ms) of a patient with abnormal motion of the left-ventricular myocardial wall. Asvide 2014;1:290. Available online: http://www.asvide.com/articles/303
62. Zhang S, Joseph AA, Voit D, Schaetz S, Merboldt KD, Unterberg-Buchwald C, Hennemuth A, Lotz J, Frahm J. Real-time cardiac MRI with T1 contrast (3 T, 33 ms) of a patient with diastolic dysfunction during Valsalva maneuver. Asvide 2014;1:291. Available online: http://www.asvide.com/articles/304
63. Chitiboi T, Hennemuth A, Tautz L, Huellebrand M, Frahm J, Linsen L, Hahn H. Context-based segmentation and analysis of multi-cycle real-time cardiac MRI. IEEE Int Symp Biomed Imaging 2014;11:943-6.
64. Greenfield JC Jr, Cox RL, Hernández RR, Thomas C, Schoonmaker FW. Pressure-flow studies in man during the Valsalva maneuver with observations on the mechanical properties of the ascending aorta. Circulation 1967;35:653-61.

65. Parisi AF, Harrington JJ, Askenazi J, Pratt RC, McIntyre KM. Echocardiographic evaluation of the Valsalva Maneuver in healthy subjects and patients with and without heart failure. Circulation 1976;54:921-7.
66. Zhang S, Joseph AA, Voit D, Schaetz S, Merboldt KD, Unterberg-Buchwald C, Hennemuth A, Lotz J, Frahm J. Real-time cardiac MRI with T1 contrast (3 T, 33 ms) of a patient with mild aortic insufficiency: 3-chamber view. Asvide 2014;1:292. Available online: http://www.asvide.com/articles/305
67. Zhang S, Joseph AA, Voit D, Schaetz S, Merboldt KD, Unterberg-Buchwald C, Hennemuth A, Lotz J, Frahm J. Real-time cardiac MRI with T1 contrast (3 T, 33 ms) of a patient with mild aortic insufficiency: coronal view (same as in Figure 16). Asvide 2014;1:293. Available online: http://www.asvide.com/articles/306
68. Zhang S, Joseph AA, Voit D, Schaetz S, Merboldt KD, Unterberg-Buchwald C, Hennemuth A, Lotz J, Frahm J. Real-time phase-contrast flow MRI (3 T, 37 ms) of a patient with mild aortic insufficiency: magnitude images (same as in Figure 16). Asvide 2014;1:294. Available online: http://www.asvide.com/articles/307
69. Zhang S, Joseph AA, Voit D, Schaetz S, Merboldt KD, Unterberg-Buchwald C, Hennemuth A, Lotz J, Frahm J. Real-time phase-contrast flow MRI (3 T, 37 ms) of a patient with mild aortic insufficiency: phase-contrast maps (same as in Figure 16). Asvide 2014;1:295. Available online: http://www.asvide.com/articles/308

Cite this article as: Zhang S, Joseph AA, Voit D, Schaetz S, Merboldt KD, Unterberg-Buchwald C, Hennemuth A, Lotz J, Frahm J. Real-time magnetic resonance imaging of cardiac function and flow—recent progress. Quant Imaging Med Surg 2014;4(5):313-329. doi: 10.3978/j.issn.2223-4292.2014.06.03

